Journal of Photochemistry & Photobiology, B: Biology 154 (2016) 67–76

Contents lists available at ScienceDirect

Journal of Photochemistry & Photobiology, B: Biology

journal homepage: www.elsevier.com/locate/jphotobiol

Novel bio-essential metal based complexes linked by heterocyclic ligand: Synthesis, structural elucidation, biological investigation and docking analysis

T. Arun [a], R. Subramanian [b], N. Raman [a,*]

[a] Research Department of Chemistry, VHNSN College, Virudhunagar 626 001, Tamilnadu, India
[b] Centre for Scientific and Applied Research, PSN College of Engineering and Technology, Tirunelveli 627152, Tamilnadu, India

ARTICLE INFO

Article history:
Received 7 October 2015
Received in revised form 6 November 2015
Accepted 10 November 2015
Available online 3 December 2015

Keywords:
Heterocyclic ligand
DNA binding
DNA cleavage
Anti-microbial activity
Docking analysis

ABSTRACT

New series of bio-essential metal based complexes linked by Schiff base ligand (L) and 2,2′-bipyridine (bpy) have been synthesized and characterized by diverse spectral techniques such as elemental analysis, magnetic susceptibility, molar conductivity measurements, FT-IR, UV–Vis., ^{1}H NMR, ^{13}C NMR, EPR and Mass. The spectral data suggest that the metal complexes espouse octahedral geometry around the metal ions. Interactions of the complexes with CT DNA have been explored by electronic absorption, ethidium bromide displacement assay, viscosity measurements, cyclic voltammetry and differential pulse voltammetry in order to evaluate the possible DNA-binding mode and to calculate the corresponding DNA-binding constants. The DNA interaction studies propose that the intercalative mode of interaction and the complexes exhibit oxidative cleavage of pUC19 DNA in the presence of hydrogen peroxide as activator. The synthesized Schiff base ligand and its metal complexes have been screened for anti-microbial activity by micro dilution method against two Gram-positive bacteria (*Staphylococcus aureus* and *Bacillus subtilis*), two Gram-negative bacteria (*Escherichia coli* and *Salmonella typhi*) and three fungi strains (*Fusarium solani*, *Aspergillus niger* and *Candida albicans*) revealing that the complexes are good anti-pathogenic agents than the ligand. Moreover, molecular docking analysis has been performed to confirm the nature of binding of the complexes with DNA.

1. Introduction

Schiff bases are vital class of ligands due to their synthetic flexibility, selectivity and sensitivity towards the central metal atom. These ligands are considered as 'privileged' ligands in coordination chemistry due to simple preparation by the condensation process of primary amines and an aldehyde [1,2]. Schiff base ligands containing azomethine (—HCN) group is particularly suited for coordination of metal ions via N-atom of the lone pair. Recently, these ligands have received much consideration mainly because of their wide application in the field of optical materials [3], catalysis [4], drug design, biological probes [5] and used as chemical sensor [6]. The Schiff base ligands with nitrogen and oxygen donor sites in their structures act as good chelating agents for the transition metal ions. Coordination of Schiff bases with metal ions such as copper, cobalt, nickel and zinc, often enhances their activities [7]. Moreover, the complexes of Schiff bases showed promising biological activity including antitumor, antibacterial, antifungal, herbicidal, medical imaging, and biological modeling applications [8–10].

The important function of DNA in living process is that it acts as storage and transporter of genetic information in a cell and also the most important intercellular target of anticancer drugs [11,12]. The different sequences present in the DNA are concerned in various regulatory progression such as gene expression, gene transcription, mutagenesis and carcinogenesis etc. [13]. These progressions can be modified by the interaction of metal complexes with DNA leading to DNA damage. More recently, Shahabadi et al., have reported that the interaction between the small molecules and DNA can cause DNA damage. Further, it blocks the division of cancer cells resulting in cell death [14,15]. For these reasons, exploring and designing of novel metal based complexes capable of interacting with DNA are necessary nowadays. Metal complexes interact with DNA duplex generally by variety of binding modes such as non-covalent and covalent interactions [16]. In the non-covalent interactions, intercalation is one of the most predominant binding sites owing to its various application in anti-tumor and molecular biology [17].

On the basis of the above stated facts, the synthesis of new Schiff base from 3,4-dimethoxybenzaldehyde and *o*-phenylenediamine has been reported. The Schiff base ligand has been coordinated to bio-essential transition metal ions Cu(II), Co(II), Ni(II) and Zn(II) to form the mixed ligand complexes using 2,2′-bipyridine as ancillary ligand.

* Corresponding author.
E-mail address: ramanphotochem@gmail.com (N. Raman).

http://dx.doi.org/10.1016/j.jphotobiol.2015.11.011
1011-1344/

Further, the ligand and metal complexes have been characterized successfully by physicochemical and various spectroscopic techniques. The bio-relevancy of these complexes have been efficiently examined and explored by DNA binding, DNA cleavage and anti-microbial studies. Finally, the docking analysis has been executed to confirm the mode of binding of complexes with DNA.

2. Experimental

2.1. Materials

The chemicals involved in this work were of AnalaR grade and were used without further purification. 3,4-dimethoxybenzaldehyde, *o*-phenylenediamine and 2,2′-bipyridine (bpy) were obtained from Sigma Aldrich. Calf thymus DNA (CT DNA) (Himedia, India) and pUC19 plasmid DNA (Bangalore Genei, India) were used for DNA binding and cleavage studies. All other chemicals, solvents and metal salts were procured from E-Merck, India.

2.2. Physical Measurements

Elemental analysis (C, H and N) data were obtained using a Perkin-Elmer 240 elemental analyzer. Vibration spectra were performed on FTIR–Shimadzu model IR-Affinity-1 spectrophotometer using KBr discs. The NMR spectra of the ligand and Zn(II) complex were recorded on a Bruker Advance DRX 300 spectrometer operating at room temperature (RT). RT magnetic susceptibility measurements were carried out on a modified Gouy-type magnetic balance, Hertz SG8-5HJ. The molar conductivity of the complexes in DMSO solution (10^{-3} M) was measured in a deep vision 601 model digital conductometer at RT. The EPR spectrum was accomplished at liquid N_2 temperature (77 K) using tetracyanoethylene (TCNE) as the g-marker. Shimadzu Model 1601 UV–Visible spectrophotometer and Hitachi F–2500 fluorescence spectrophotometer were employed to attain the electronic and fluorescence spectra, respectively. Cyclic voltammetric (CV) experiments were achieved on a CHI 620C electrochemical analyzer in freshly distilled DMSO solution.

2.3. Synthesis of Schiff Base (L)

For the synthesis of Schiff base ligand (L), an ethanolic solution of 3,4-dimethoxybenzaldehyde (0.2 mM) was added to an ethanolic solution of *o*-phenylenediamine (0.1 mM) and the resultant mixture was refluxed for 4 h. The solid product formed was filtered, washed and recrystallized from ethanol, dried *in vacuo*.

[L] Yield: 76%; yellow color; Anal. Calc.(%): C (71.2), H (5.9) and N (6.9); Found (%): C (70.1), H(5.4) and N (6.5); FT-IR (KBr) (cm^{-1}): 1608 (—HCN), 2880–2920 (C—H) and 1400–1600 (CC); ^{1}H NMR (DMSO-d_6) δppm: (Ar–H) 6.4–7.5(m), (—CHN) 8.6(s), and (—O-CH_3) 3.4(s) ppm; ^{13}C NMR (DMSO-d_6): δppm 119.0–146.2 (Ar–C), 159.7 (—CHN) and 53.4 (—O-CH_3) ppm; UV–Vis. in DMSO, nm (transition): 254 (π–π*) and 370 (n-π*)

2.4. Synthesis of Metal Complexes

To synthesize metal complexes, an equimolar mixture of Schiff base ligand (L) (0.1 mM), metal chloride (0.1 mM) and 2,2′-bipyridine (0.1 mM) was mixed in a portion of ethanol (40 mL) and the resultant mixture was refluxed for 8 h. The resultant product was washed with ethanol and then recrystallized. The obtained solid product was filtered, dried in vacuo at 60 °C and kept in a desiccator.

[$CuL(bpy)Cl_2$]: Yield: 69%; brown color; Anal. Calc.(%): C (58.7), H (4.6), N (8.1) and Cu (9.1); Found (%): C (57.2), H (4.3), N (7.6) and Cu (8.3); FT-IR (KBr) (cm^{-1}): 1598 (—CHN), 1586 (—CN) (bpy), 376 (M–Cl) and 454 (M–N); $\wedge_m$ (Ω^{-1} mol^{-1} cm^2) 12.4; μ_{eff} (BM) 1.81; UV–Vis. in DMSO, nm (transition): 410 (LMCT) and 620 (d–d).

[$CoL(bpy)Cl_2$]: Yield: 71%; brown color; Anal. Calc.(%): C (59.1), H (4.6), N (8.1) and Co (8.5); Found (%): C (58.2), H (4.2), N (7.6) and Cu (7.8); FT-IR (KBr) (cm^{-1}): 1595 (−CH = N), 1592 (−C = N) (bpy), 354 (M-Cl) and 420 (M-N); $\wedge_m$ (Ω^{-1} mol^{-1} cm^2) 8.3; μ_{eff} (BM) 4.63; UV–Vis. in DMSO, nm (transition): 388 (LMCT) and 560 (d–d).

[$NiL(bpy)Cl_2$]: Yield: 64%; yellow color; Anal. Calc (%): C (59.1), H (4.6), N (8.1) and Ni (8.5); Found (%): C (57.3), H (4.1), N (7.5) and Ni (8.2); FT-IR (KBr) (cm^{-1}) 1602 (−C = N), 1588 (−C = N) (bpy), 367 (M-Cl) and 434 (M-N); $\wedge_m$ (Ω^{-1} mol^{-1} cm^2) 7.2; μ_{eff} (BM) 3.28; UV–Vis. in DMSO, nm (transition): 407 (LMCT) and 710 (d–d).

[$ZnL(bpy)Cl_2$]: Yield: 68%; greenish yellow color; Anal. Calc (%) C (58.5), H (4.6); N (8.0) and Zn (9.3); Found (%): C (57.6), H (4.2), N (7.8) and Zn (8.7); FT-IR (KBr) (cm^{-1}): 1598 (—CHN), 15,854 (CN) (bpy), 362 (M–Cl) and 438 (M–N); ^{1}H NMR (DMSO-d_6) δppm: (Ar–H) 6.4–7.5 (m), (—CHN) 8.5 (s) and (—O-CH_3) 3.4 (s) ppm; ^{13}C NMR (DMSO-d_6): δppm 119.0–146.2 (Ar–C), 158.4 (—CHN), 153.3 (—CN) and 53.4 (—O-CH_3) ppm; $\wedge_m$ (Ω^{-1} mol^{-1} cm^2) 16.4; μ_{eff} (BM) diamagnetic; UV–Vis. in DMSO, nm (transition): 380 (LMCT).

2.5. Biological Evaluation

The methods used in the biological evaluation (DNA binding, DNA cleavage and antimicrobial screening) are detailed in supplementary file.

2.6. Docking Analysis

Docking analysis of L and its metal complexes have been performed using HEX 6.3 software which is an interactive molecular graphics program for the interaction, docking calculations and to identify possible docked poses of the biomolecules. The crystal structure of DNA duplex of sequence d(CGCGAATTCGCG)$_2$ dodecamer (PDB ID: 1BNA) is downloaded from the protein data bank.

3. Results and Discussion

New bio-essential metal based complexes were synthesized from Schiff base ligand (L) and 2,2′-bipyridine. L and derived complexes are found to be stable over the extended periods. These complexes have been characterized by spectral techniques such as FT-IR, UV–visible, ^{1}H NMR, ^{13}C NMR, EPR, Mass, elemental analysis, magnetic susceptibility and molar conductivity measurements. L is soluble in common organic solvents whereas metal complexes are only soluble in DMF and DMSO.

3.1. Elemental Analysis and Molar Conductivity Measurements

The general synthetic pathway for the heterocyclic Schiff base ligand (L) and its mixed ligand metal complexes is given in Scheme 1. The very similarity between the obtained elemental analysis data of L and the metal complexes suggests the stoichiometry, [$ML(bpy)Cl_2$]. The DMSO solution of the metal complexes shows lower molar conductance values (7.2–16.4 Ω^{-1} cm^2 mol^{-1}) which might be due to the non-electrolytic nature of the complexes.

3.2. FT-IR Spectra

The FT-IR spectra of ligand (L) and metal complexes were compared and shown in Fig. S1. The IR spectrum of ligand (L) [Fig. S1(a)], shows

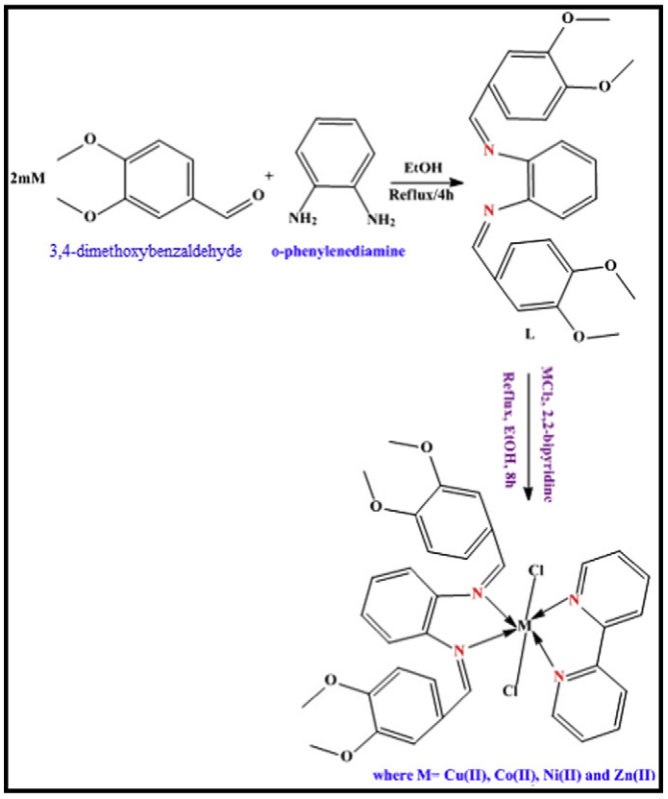

Scheme 1. Schematic route for the synthesis of Schiff base (—HCN) ligand (L) and its metal complexes.

the strong band acquired at ~1608 cm^{-1}, due to azomethine stretching vibration (—CHN) acquired in the ligand, indicating that condensation between 3,4-dimethoxybenzaldehyde and *o*-phenylenediamine has taken place, resulting in the formation of desired Schiff base ligand. It was also confirmed by the significant aromatic —CC-stretch, which acquired at ~1487 cm^{-1} as a medium band. On complexation [Fig. S1(b–d)] a major shift in azomethine (—CHN) linkage to lower frequency by ~10–15 cm^{-1}, and a new band acquired in the range ~1595–1602 cm^{-1} suggesting the involvement of the azomethine —N to the metal ions [18]. This observation is further supported by M–N characteristic peak noted at ~420–454 cm^{-1} in all the complexes. The coordination of 2,2′-bipyridine to the metal ions can be confirmed by the existence of new characteristic (—CN-) peaks in all the complexes. As expected, such (—CN) band acquired in the region ~1584–1592 cm^{-1}, and it indicates the coordination of 2,2′-bipyridine to the metal ions [19]. In addition, the IR spectra of all the synthesized complexes show another band at ~354–376 cm^{-1}, which shows the successful coordination of chlorine to the metal ions. Thus FT-IR spectral studies assure the formation of L and the complexes which have 2,2′-bipyridine as the ancillary ligand.

3.3. UV–Vis. Spectroscopy

The UV–Vis. spectra of the Schiff base ligand (L) and its metal complexes recorded in DMSO solution are given in Fig. S2. In the UV spectrum of ligand (L) [Fig. S2(a)], notably two characteristic absorption bands are observed. The emergence of higher energy absorbtion band at 254 nm can be attributed to the π–π* transition of π electrons present in aromatic phenyl ring (CC) and azomethine chromophores. The observed lower energy absorption band at 370 nm, is due to the n–π* transition of non-bonded electrons available in (—CHN) groups. Furthermore, the UV–Vis. spectra of the complexes displayed the characteristic of π–π* and n–π* transition bands below 370 nm, but they slightly differ in their wavelength or absorption, which may be due to the coordination of ligand to the metal ions. The charge transfer (Metal to ligand) transition can also be identified around ~430 nm in UV spectra of all the metal complexes [20]. However, metal complexes reveal an extra and much important characteristic band that appears as the result of d–d transition. This d–d transition is very helpful to forecast the geometry of the metal complexes. The electronic spectrum of [CuL(bpy)Cl_2] displays the d–d transition band in the region 620 nm, which is due to $^2E_g \rightarrow {}^2T_{2g}$ transition. This d–d transition band powerfully favors a distorted octahedral geometry around the metal ions [21]. The electronic spectrum of [CoL(bpy)Cl_2] shows this d–d transition $^4T_{1g}(F) \rightarrow {}^4T_{2g}(F)$ at 560 nm as the result of octahedral geometry [22]. The absorption spectrum of [NiL(bpy)Cl_2], displays two d–d transition bands in the region 570 and 690 nm, which are assigned to $^3A_{2g}(F) \rightarrow {}^3T_{2g}(F)$, and $^3A_{2g}(F) \rightarrow {}^3T_{1g}(F)$, transitions respectively, which confirms the octahedral geometry of the complexes [23].

3.4. ^1H NMR and ^{13}C NMR Spectra

The ^1H NMR spectra of the Schiff base ligand (L) and its [ZnL(bpy)Cl_2] complex have been recorded in $CDCl_3$. The obtained ^1H NMR spectra of Schiff base ligand (L) and [ZnL(bpy)Cl_2] complex are illustrated in supplementary file (Fig. S3). The ^1H NMR spectrum of ligand (L) exhibits singlet at 8.6 (s) ppm due to azomethine protons (—CHN) of Schiff base ligand. Moreover, the ligand exhibits the following signals: phenyl multiplet at 6.4–7.5 (m) ppm and methoxy protons (—O-CH_3) at 3.4 (s) ppm. In the case of [ZnL(bpy)Cl_2], such distinctive peak of azomethine group (—CHN) gets shifted to upfield region at 8.5 (s) ppm, which confirms the coordination of azomethine group(—CHN) with Zn(II) metal ion [24]. There is no appreciable change in all other signals of the complexes.

The ^{13}C NMR spectrum of L exhibits aromatic carbon signals between 119.0 and 146.2 ppm. It also exhibits the other important peaks at 159.7 and 53.4 ppm, characteristic of —HCN and methoxy (−O-CH_3) carbon. In the case of [ZnL(bpy)Cl_2], such characteristic peak of —HCN bond gets shifted to 158.4 ppm and a new peak is also seen at 154.3 due to the 2,2′-bipyridine (—CN) carbon. This evidence of 2,2′-bipyridine (—CN) carbon greatly supports the coordination with metal center.

3.5. EPR Spectra

EPR spectroscopy has been recognized as the most excellent technique to investigate the metal ion environment in the complexes, i.e., the geometry and nature of the bonding between the metal ion and its ligands, in particular Cu(II) complexes. In the present study, EPR spectrum of [CuL(bpy)Cl_2] was performed. The recorded EPR spectrum of [CuL(bpy)Cl_2] is given in supplementary file (Fig. S4). It exposed two g factors $g_{||}$ and $g_{\perp}$. The calculated spin Hamiltonian spectral data of [CuL(bpy)Cl_2] are listed in supplementary file (Table S1). From this spectral data, it is found that $g_{||}$ (2.11) > $g_{\perp}$ (2.02) > g_e (2.0023) which indicates the unpaired electron is present in the $d^2_{x^2-y^2}$ orbital and it is likely to be octahedral geometry as conferred in UV–Vis. spectroscopy [25]. The $g_{||}$ value of Cu(II) complex can be used as a measure of the covalent character of the metal–ligand interactions. If the value is more than 2.3, the metal–ligand bond is essentially ionic and the value less than 2.3 is indicative of covalent character. In the present EPR results, lesser value of $g_{||}$ (2.11) is compared to 2.3 which is a good evidence for the covalent character of Cu–Nitrogen interactions, as suggested by Kivelson and Neiman [26]. From the values of g factors, the exchange coupling factor (G) can be expressed by the following equation:

$$G = \left(g_{||} - 2\right)/\left(g_{\perp} - 2\right)$$

It has been already reported that, if G > 4.0, the local tetragonal axes are aligned parallel or slightly misaligned. If G < 4.0, significant

exchange coupling might be present and considerable misalignment will be there. In this study, the observed G value of $[CuL(bpy)Cl_2]$ is 5.5 which means that the local tetragonal axes are aligned parallel or slightly misaligned and exchange coupling could be negligible [27]. The observed empirical ratio of $g_{||}/A_{||}$ value for the $[CuL(His)_2]$ is 162 which indicates the octahedral geometry of $[CuL(bpy)Cl_2]$ with small distortions.

3.6. Mass Spectra

The mass spectra of the Schiff base ligand (L) and its $[CuL(bpy)Cl_2]$ complex are given in supplementary file (Fig. S5). The mass spectrum of Schiff base ligand (L) showed molecular ion peak at m/z = 138 corresponding to $[C_8H_9O_2]^+$ ion. In addition, the ligand (L) exhibits peaks for the fragments at m/z 241, 165 and 106 corresponding to $[C_{15}H_{14}NO_2]^+$, $[C_9H_{10}O_2N]^+$ and $[C_7H_6O]^+$ respectively (Fig. S3a). Moreover, the mass spectrum of $[CuL(bpy)Cl_2]$ complex showed peaks with m/z 659 (Base peak), 557, 539, 468, 405, 289 and 218 corresponding to $[C_{34}H_{32}ClCuN_4O_4]^+$, $[C_{26}H_{23}Cl_2CuN_4O_2]^+$, $[C_{24}H_{24}Cl_2CuN_2O_2]^+$, $[C_{24}H_{24}CuN_2O_4]^+$ $[C_{24}H_{24}N_2O_4]^+$, $[C_{10}H_8Cl_2CuN_2]^+$ and $[C_{10}H_8CuN_2]^+$ respectively (Fig. S3b). The m/z of all the fragments of ligand (L) and its metal complex prove the stoichiometry of the complexes of the type $[ML(bpy)Cl_2]$. The mass spectra of ligand (L) and its complexes show molecular ion peaks which are in good agreement with the structure suggested by elemental analysis, magnetic and spectral studies.

3.7. Biological Studies

In order to confirm the possible binding mode of the complexes with CT DNA, many techniques were used. The DNA cleavage and antipathogenic screening experiments have also been carried out. In addition to that, molecular docking calculations have been performed to understand the nature of binding of the complexes with DNA. They are discussed below.

3.7.1. Electronic Absorption Titrations

Electronic absorption titration is an effectual method to examine the binding mode and the binding affinity of metal complexes with DNA. It is generally accepted that the interaction of metal complexes with DNA generally takes place via both covalent and non-covalent ways. In case of covalent interaction, the labile ligand of the complexes is replaced by nitrogen base of DNA such as guanine N7 while the non-covalent DNA binding with intercalative, electrostatic and groove binding of metal complexes arise in the outside of DNA double helix [28]. The absorption spectra of the metal complexes in the presence and absence of DNA are given in Fig. 1. As shown in Fig. 1, the complexes displayed absorption bands around 300–309 nm, assigned to intraligand transition. Upon increasing amounts of DNA, the absorption bands of the complex were affected. In specific hypochromism and red shift were obtained in all the complexes after escalating DNA concentration. While escalating DNA concentration, the observed hypochromisms are 12.4%, 8.7%, 9.3% and 7.2% for $[CuL(bpy)Cl_2]$ (309 nm), $[CoL(bpy)Cl_2]$ (304 nm), $[NiL(bpy)Cl_2]$ (306 nm) and $[ZnL(bpy)Cl_2]$ (305 nm) respectively. These considerable hypochromism and red shifts reveal that complexes can interact with CT DNA through intercalation mode of binding which may occur by the strong stacking interaction between the aromatic chromophore of the ligand and the base pairs of DNA [29].

In order to compare the CT DNA-binding strength of the studied complexes quantitatively, their intrinsic binding constants were evaluated by the changes associated with absorption for the complexes with increasing amounts of CT DNA. The electronic absorption data are given in Table 1. The determined intrinsic binding constants for $[CuL(bpy)Cl_2]$, $[CoL(bpy)Cl_2]$, $[NiL(bpy)Cl_2]$ and $[ZnL(bpy)Cl_2]$ are $3.24 \times 10^6\ M^{-1}$, $2.55 \times 10^6\ M^{-1}$, $2.28 \times 10^6\ M^{-1}$ and $2.08 \times 10^6\ M^{-1}$, respectively. Interestingly, the observed K_b value of the present organometallic complexes is lower than that for a classical intercalator, such as EB and higher than those of some Schiff base metal complexes [30] indicating that the present complexes strongly bind with DNA through an intercalation mode at the double helix structure of DNA.

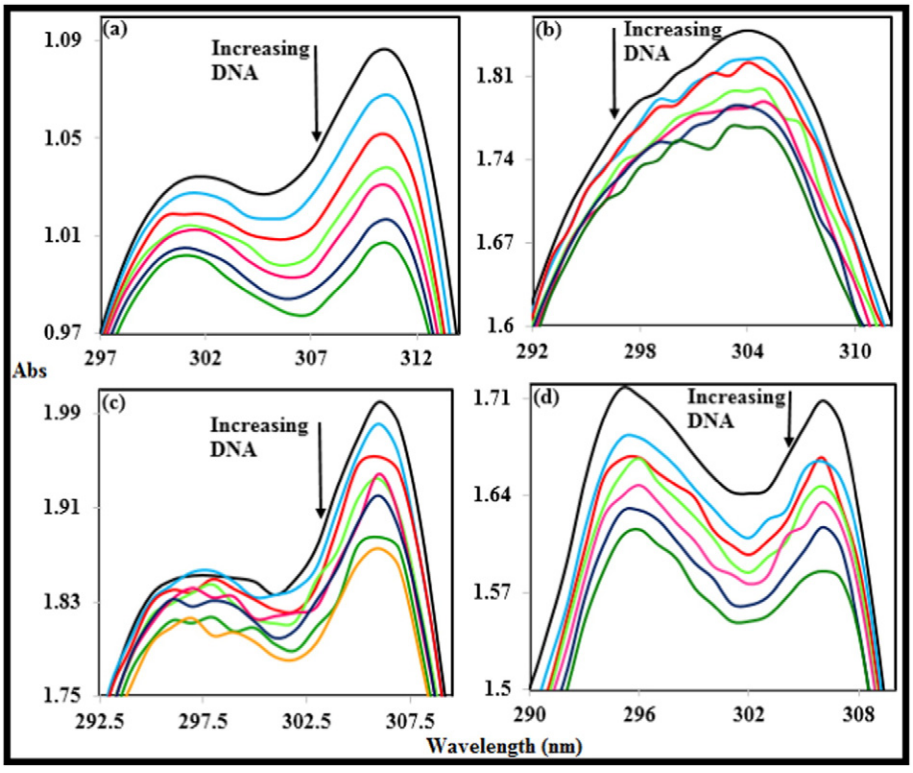

Fig. 1. Absorption spectra of (a) $[CuL(bpy)Cl_2]$, (b) $[CoL(bpy)Cl_2]$, (c) $[NiL(bpy)Cl_2]$ and $[ZnL(bpy)Cl_2]$ complexes in buffer pH = 7.2 at 25 °C in the presence of increasing amount of DNA. Arrow indicates the changes in absorbance upon increasing the DNA concentration.

3.7.2. EB Fluorescence Displacement Assay

In order to further confirm the intercalation mode between the complexes with DNA has been studied by EB fluorescence displacement assay. EB is one the most sensitive fluorescent probes, does not have any appreciable emission intensity in Tris–HCl-buffer solutions, due to fluorescence quenching of free EB by the solvent molecules. Wilson et al., have been reported that EB is a distinctive indicator of intercalation while it can show enhanced emission intensity in the presence of DNA, due to its strong intercalation of the planar of EB phenanthridine ring between the adjacent base pairs of DNA [31]. This enrichment of fluorescence intensity can be quenched by the addition of another molecule, which can bind DNA via intercalative mode by displacing EB. The EB fluorescence displacement spectra of EB bound to DNA both in the absence and presence of $[CuL(bpy)Cl_2]$ and $[NiL(bpy)Cl_2]$ are shown in Fig. 2. Upon increasing amount of complex to the EB-bound DNA causes a slow decrease in fluorescence intensity due to interaction between the complexes and EB-DNA and it further leads to the quenching in the fluorescence intensity of EB-DNA system. The reason for the decrease in emission intensity is the replacement of EB from EB-DNA system by metal complexes. It suggests the intercalative mode of binding [32]. Fluorescence quenching data were further analyzed by means of the following Stern–Volmer equation,

$$I_0/I = 1 + K_{sv}[Q]$$

where I_0 and I are the fluorescence intensities in the absence and presence of quencher, respectively; [Q] is the concentration of the quencher; K_{sv} is the Stern–Volmer quenching constant, which is obtained from the slope of plot (I_0/I *vs* [Q]). The quenching constant (Ksv) values of the metal complexes are $2.08 \times 10^4\ M^{-1}$ and $1.27 \times 10^4\ M^{-1}$, respectively. The results are consistent with the absorption spectral studies.

3.7.3. Viscosity Measurements

The mode of binding between the complexes and DNA was also confirmed by viscosity measurements. The previous report explains that, in classical intercalation, the intercalating agents (e.g., EtBr) are expected to elongate the DNA double helix and base pairs are divided to accommodate the intercalated ligands and thus outcome is the enhancement of DNA's viscosity. In contrast partial or non-classical intercalation of the ligand could twist or kink the DNA double helix, reduce its effective length and decrease the viscosity [33]. Therefore, a hydrodynamic measurement such as viscosity is considered as the least ambiguous and most critical experiment for binding mode of the complexes with DNA. The changes in the viscosity of CT DNA in the presence of increasing amounts of the complexes are given in Fig. 3. As shown in this Fig. 3, ethidium bromide (EtBr) usually increases the relative viscosity due to lengthening of DNA double helix because of intercalation. Upon increasing amount of complexes the relative specific viscosities of DNA increased steadily, which is confirmed the metal complexes bound to DNA by intercalation [34].

3.7.4. Electrochemical Titrations

The transition metal complexes of high oxidation state play a crucial function in bioinorganic chemistry, because of their pharmacological importance as redox enzyme models. Cyclic and differential pulse voltammetries (CV and DPV) were also carried out on metal complexes by increasing the DNA concentration. These methods are considered to be the very sensitive analytical techniques to find out the changes in oxidation state of the metallic species in the presence of biomolecules. It has been already reported that, when the metal complexes interact with DNA via intercalation mode, the peak potential presents a positive shift. It presents a negative shift for electrostatic interaction [35]. In the present study, CV and DPV techniques have been employed to find out the nature of DNA binding mode. In all of the experiments, the binding of complexes with CT DNA were carried out in double distilled water with Tris–HCl [(hydroxymethyl)aminomethane] (Tris–HCl, 5 mM) and NaCl (50 mM) and adjusted to pH 7.2 with hydrochloric acid.

The cyclic voltammograms of $[Cu(bpy)Cl_2]$, $[Co(bpy)Cl_2]$, $[Ni(bpy)Cl_2]$ and $[Zn(bpy)Cl_2]$ have been collected both in the absence and presence of DNA. The effect of varying DNA concentration on cyclic voltammograms of the studied complexes is presented in Fig. 4. Incremental addition of DNA effectively changes both potentials and currents of anodic as well cathodic peaks. This confirms the interaction between the complex and DNA [36].

The parameters received from CV of all the metal complexes in DMSO are given in Table 2. The CV and DPV voltammograms of the complexes in 5 mM Tris HCl/50 mM NaCl buffer (pH = 7.2) were recorded in the range of +1 to −1 with scan rate of 0.1 Vs^{-1}.

In the absence of DNA, CV of $[Cu(bpy)Cl_2]$ reveals four characteristic peaks. Among them, two are anodic (E_{pa}: −0.489 and −0.668 V) and two are cathodic (E_{pc}: 0.689 and −1.068 V). From the two separate anodic and cathodic peaks, two redox couples are assumed as follows:

$$Cu(II) \rightarrow Cu(I)\ (Epa = -0.489\ V; Epc = 0.689\ V; \Delta Ep = 0.179\ V \text{ and } E_{1/2} = -0.089\ V);$$

$$Cu(I) \rightarrow Cu(0)\ (Epa = -0.668\ V; Epc = -1.068\ V; \Delta Ep = 1.759\ V \text{ and } E_{1/2} = -0.189\ V).$$

$[Co(bpy)Cl_2]$ shows only one redox couple in the absence of DNA and its details are given below:

$$Co(II) \rightarrow Co(I),\ (Epa = 1.119\ V, Epc = 0.533\ V, \Delta Ep = 0.585\ V, \text{and } E_{1/2} = 0.826\ V).$$

Likewise $[Ni(bpy)Cl_2]$ shows one redox couple in the absence of DNA and it is detailed below:

$$Ni(II) \rightarrow Ni(I),\ (Epa = 0.642\ V, Epc = -0.824\ V, \Delta Ep = 1.466\ V, \text{and } E_{1/2} = -0.090\ V).$$

CV study of $[Zn(bpy)Cl_2]$ in the absence of DNA also results in one redox couple and the details are provided below:

$$Zn(II) \rightarrow Zn(0),\ (Epa = 0.541\ V, Epc = -1.016\ V, \Delta Ep = 1.557\ V, \text{and } E_{1/2} = 0.778\ V).$$

Irrespective of the complexes, all the above redox couples are found to have approximately unity peak current ratio which is credited that the reactions of the complexes in glassy carbon are quasi-reversible redox process.

DPV of the metal complexes both in the absence and presence of DNA is given in Fig. 5. Upon mounting the amounts of DNA, the formal peak potential as well as the current intensity are reduced. The change in the potential shift is related to the ratio of binding constant:

$$E^0{}_b - E^0{}_f = 0.0591 \log\left(K_{[red]}/K_{[oxi]}\right)$$

where E^0b and E^0f are peak potentials of complex in the presence (bound) and absence (free form) of DNA, respectively. In our case, metal complexes show one electron transfer reaction during the above said redox process and value of $K_{[red]}/K_{[oxi]}$ ratio is less than unity and this value strongly favors a quasi-reversible process. The synthesized metal complexes give both the anodic and cathodic peak potential shifts (Table 2). These shifts indicate the intercalating mode of DNA binding with metal complexes [37].

Table 1
Change in electronic absorption parameters for the complexes on interaction with CT DNA in 5 mM Tris HCl/50 mM NaCl buffer (pH 7.2).

Compound	λ max		Δλ (nm)	H%	$K_b \times 10^6\ (M^{-1})$
	Free	Bound			
$[CuL(bpy)Cl_2]$	309	311	2	12.4	3.24
$[CoL(bpy)Cl_2]$	304	305	1	8.7	2.55
$[NiL(bpy)Cl_2]$	306	308	2	9.3	2.28
$[ZnL(bpy)Cl_2]$	305	306	1	7.2	2.08

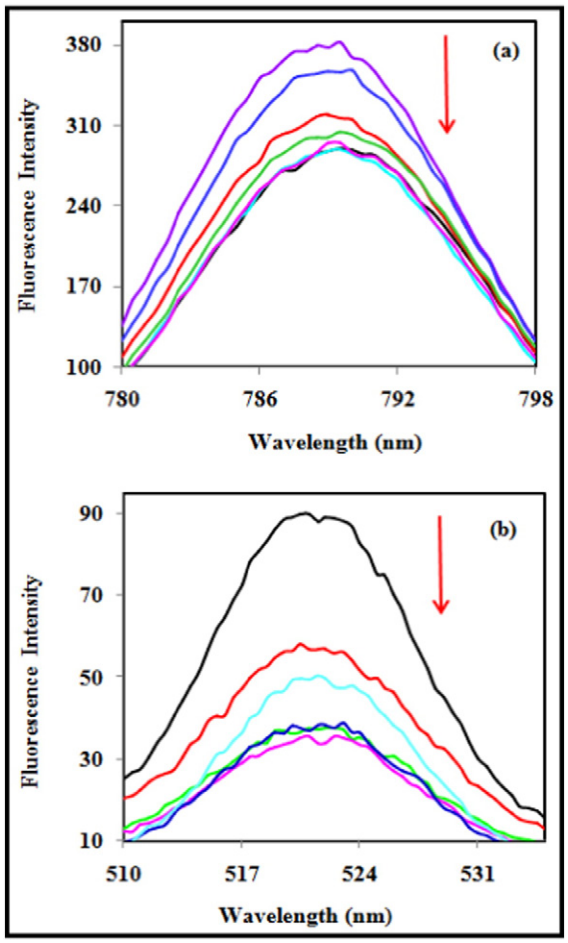

Fig. 2. Fluorescence quenching curves of EB bound to DNA: (a) [CuL(bpy)Cl_2] and (b) [NiL(bpy)Cl_2] [DNA] = 10 μL, [EB] = 5 μL, [Complex] = 0–120 μL.

3.8. DNA Cleavage Activity

The cleavage of pUC19 DNA examined by transition metal complexes has been curiosity of biochemists. This can be attained by targeting the essential components of DNA such as phospho-di-ester bonds, deoxyribose sugar moiety or nucleobases. The DNA cleavage activity of the heterocyclic ligand bridged metal complexes has been investigated by incubating the complexes with pUC19 DNA in the absence of an external agent in substrate medium of Tris–acetate–EDTA (TAE) (pH = 7.2) buffer at 37 °C by gel electrophoresis, in which migration from naturally going on, covalently closed circular form to the open circular form and linear form was scrutinized [12]. If the reaction mixture is placed under the influence of electric field, DNA is negatively charged species, it will migrate towards anode and this migration depends upon the gel concentration, size of DNA, electric potential and buffer nature. It has been already reported by Brissos et al., when pUC19 DNA is subjected to gel electrophoresis three phenomena may be observed, (I) relatively fast migration will be generated for the super coiled form (Form I): (II) if scission occurs on one strand, the super coiled system will relax to generate a slower moving open circular form (Form II): and (III) if both strands are cleaved, the linear form (Form III) will be produced, which migrates at an intermediate rate [38].

The oxidative DNA damage ability the heterocyclic ligand and its mixed ligand metal complexes is studied with pUC19 DNA in the absence and presence of H_2O_2 as an oxidizing agent. The pUC19 DNA cleavage activity of the L and its complexes has been carried out in the presence of H_2O_2 as shown in Fig. 6. The DNA cleavage activity is significantly enhanced by incorporation of metal ion in the respective oxidant. As seen from Fig. 6, the control experiments with DNA alone (Lane 1) and DNA presence of L (Lane 2) do not show any cleavage ability. However, the cleavage of super coiled (form-1) to the open circular (form-II) and liner (form-III) is migrated by all the metal complexes. These observations highlight that a combination of a metal complex and oxidant H_2O_2 is very necessary to show more efficient cleavage of DNA. This cleavage activity may be due to the formation of hydroxyl radical ($OH^{\cdot}$). The formation of hydroxyl free radical ($OH^{\cdot}$) is due to the reaction between the metal complex and oxidant. The metal complexes in the presence of H_2O_2 may produce reactive hydroxyl radical ($OH^{\cdot}$) that can damage the deoxyribose moiety [39].

3.9. Antimicrobial Screening

Biological investigations of the newly synthesized Schiff base ligand (L) and its metal complexes were screened for in-vitro anti-pathogenic activity against sensitive organisms such as two Gram-positive bacteria (*Staphylococcus aureus* and *Bacillus subtilis*), two Gram-negative bacteria (*Escherichia coli* and *Salmonella typhi*) and three fungi (*Fusarium solani*, *Aspergillus niger* and *Candida albicans*) by dilution method. Gentamicin and Fluconazole were used as standards for bacteria and fungi respectively. The minimum inhibitory concentration (MIC) values of measured in antibacterial and antifungal studies of the complexes are given in Tables 3 and 4.

The results in the above Tables 3 and 4, indicate that the inhibition growth of the Schiff base ligand becomes more enhanced when chelation with the metal ions. This enhancement in anti-pathogenic activity is rationalized on the basis of the metal chelates by possessing an additional azomethine (HCN) linkage which imports in elucidating the mechanism of transamination and resamination reactions in

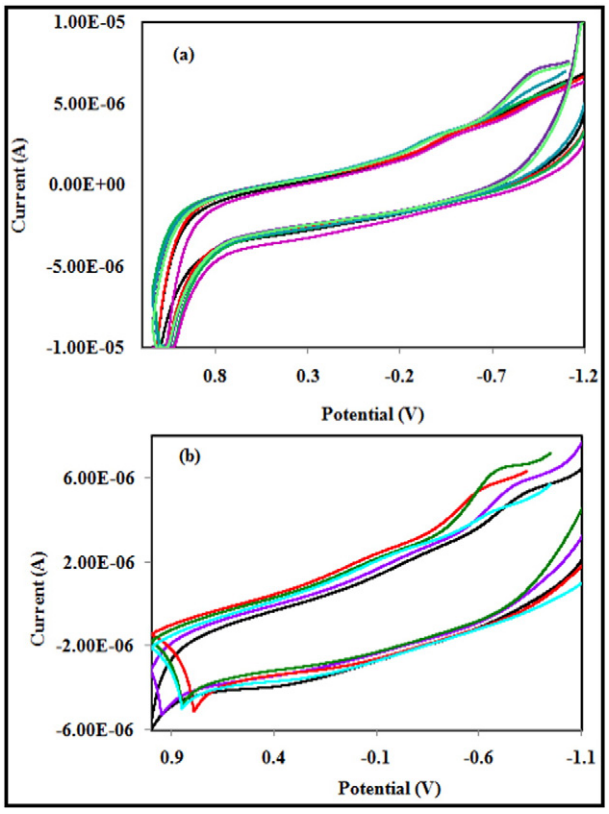

Fig. 3. Cyclic voltammograms of (a) $[CuL(bpy)Cl_2]$ and (b) $[NiL(bpy)Cl_2]$ in buffer (pH = 7.2) at 25 °C in the presence of increasing amount of DNA.

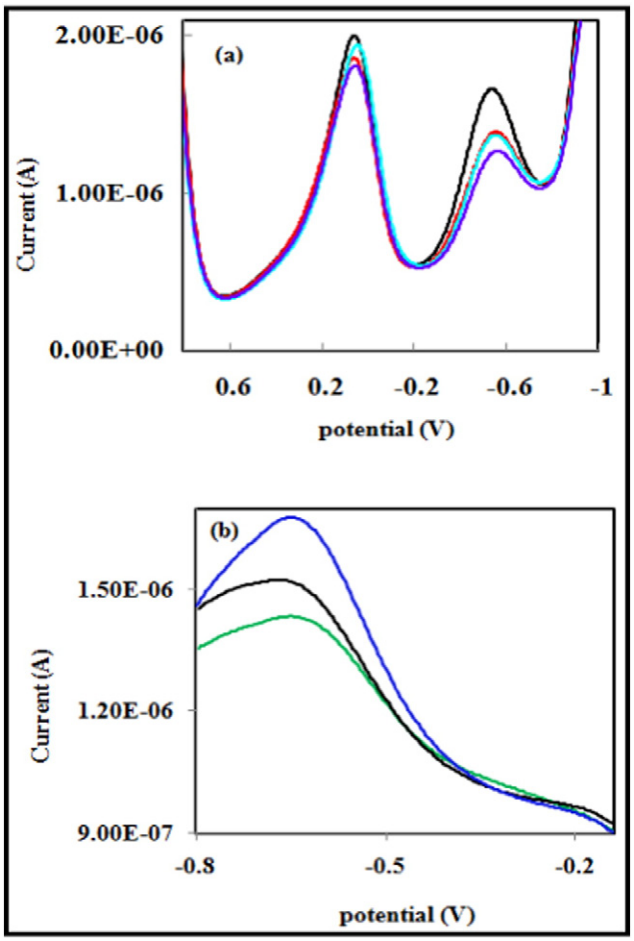

Fig. 4. Differential pulse voltammograms of (a) $[CuL(bpy)Cl_2]$ and (b) $[CoL(bpy)Cl_2]$ in buffer (pH = 7.2) at 25 °C in the presence of increasing amount of DNA.

biological system. Moreover, the presence of azomethine group (—CHN) and chelation effect with central metal enhances the anti-pathogenic activity [40]. This increasing anti-pathogenic activity of these mixed ligand metal complexes may be explained by Overtone concept and Tweedy's chelation theory [41]. On chelation, the polarity of the metal ion gets reduced to a greater extent, due to the overlap of the ligand orbital and partial sharing of its positive charge with donor groups. In addition, it enhances the π-electron delocalization on the whole chelating ring which results enhance in the liphophilicity of the complexes. Consequently, the metal complexes easily penetrate into the lipid membrane and blocking of the metal binding sites in the enzymes of organisms. While chelation is not the only criterion for anti-pathogenic activity, there are other several factors which also increase the activity are nature of metal ion, ligand, geometry of the metal complexes, the lipophilicity and the presence of co-ligands, the steric and pharmacokinetic factors. These mixed ligand metal complexes also disturb the respiration process of the cell wall and thus block the synthesis of the proteins which restricts further growth of organisms. From the antimicrobial results, it is observed that the Gram-positive bacteria are more sensitive to metal complexes than Gram-negative bacteria. It is due to the presence of cell wall in Gram-negative bacteria which is impermeable lipid based bacterial outer membrane.

3.10. Molecular Docking with DNA

Molecular docking is an effective technique to know the drug–nucleic acid interactions for the progress of modern drug design and finding, as well as to find out the accurate binding site available at the molecular target DNA predominantly in a non-covalent interaction [42]. Computer aided molecular docking studies of Schiff base ligand (L) and metal complexes with DNA duplex of sequence *d*(CGCGAATT CGCG)$_2$ dodecamer (PDB ID: 1BNA) were carried out in order to offer the suitable binding site and preferred orientation of the molecules inside DNA [43]. It is universally accepted that, if the binding free energy is low, then the binding affinity is more potent in between the receptor (DNA) and "the ligand" (Schiff base and its metal complexes) molecules. For these reasons, molecular docked model calculations were presented and the most probable molecular docked poses are depicted in Fig. 7. This figure obviously shows that the Schiff base ligand and its metal complexes interact with DNA through an intercalation mode involving outside edge stacking interaction with oxygen atom of the phosphate backbone. As seen from Fig. 7, it is clear that the L and metal complexes fit well into the intercalation mode of targeted DNA [44]. Moreover, resulting structures are stabilized by van der Waals interaction and hydrophobic contacts [45] with DNA functional group that define the stability of intercalations. The resulting docking scores of molecular docked L and metal complexes are found to be −226.30 (L), −270.12 $[CuL(bpy)Cl_2]$, −269.85 $[CoL(bpy)Cl_2]$, −269.69 $[NiL(bpy)Cl_2]$ and −269.57 $[ZnL(bpy)Cl_2]$ KJ mol^{-1} respectively. It is fascinating to note

Table 2
Redox potential profiles for interaction of DNA with metal complexes.

Compound	$E_{1/2}(V)^a$		$^b\Delta Ep(V)$		Ip_a/Ip_c	$K[red]/K[oxd]$
	Free	Bound	Free	Bound		
$CuL(bpy)Cl_2]$	−0.089	0.482	0.179	0.965	0.76	0.654
	−0.189	−0.061	1.759	1.782	0.89	
$[CoL(bpy)Cl_2]$	0.826	0.832	0.585	0.482	0.96	0.546
$[NiL(bpy)Cl_2]$	−0.090	0.351	1.466	2.011	0.82	0.364
$[ZnL(bpy)Cl_2]$	0.778	0.912	1.557	1.627	0.69	0.327

Data from cyclic voltammetric measurements: $^aE_{1/2}$ is calculated as the average of anodic (E_{Pa}) and cathodic (E_{pc}) peak potentials; $E^a_{1/2} = E_{Pa} + E_{pc}/2$; $^b\Delta Ep = E_{pa} - E_{pc}$.

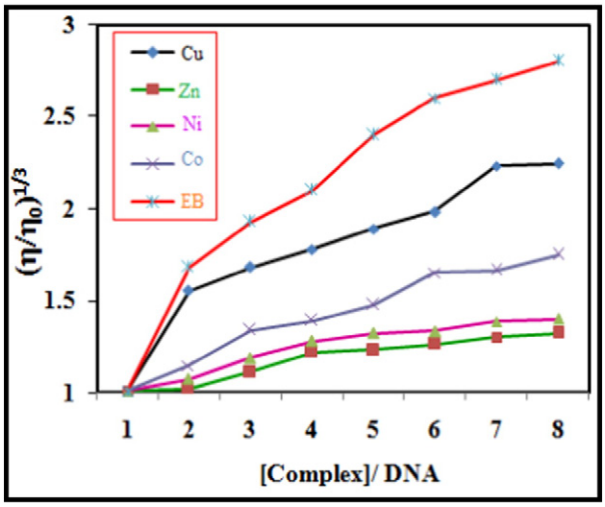

Fig. 5. Effect of increasing amounts of [EB] (⁎), [CuL(bpy)Cl_2] (♦), [CoL(bpy)Cl_2] (×), [NiL(bpy)Cl_2] (▲) and [ZnL(bpy)Cl_2] (■) on the relative viscosity of CT DNA. Plot of relative viscosity $(\eta/\eta o)^{1/3}$ *vs* [complex]/[DNA].

Table 3
Minimum inhibitory concentration of the synthesized compounds against the growth of bacteria (μM). Minimum inhibitory concentration (MIC) ($\times 10^4$ μM).

Compound	*S. aurous*	*B. subtilis*	*E. coli*	*S. typhi*
[L]	16.2	17.9	16.5	18.8
[CuL(bpy)Cl_2]	5.8	6.2	6.6	7.1
[CoL(bpy)Cl_2]	6.2	7.1	8.2	8.3
[NiL(bpy)Cl_2]	7.1	7.4	8.2	8.4
[ZnL(bpy)Cl_2]	8.1	8.4	8.7	9.3
Gentamicin	3.1	3.4	3.9	4.1

Table 4
Minimum inhibitory concentration of the synthesized compounds against the growth of fungi (μM).Minimum inhibitory concentration (MIC) ($\times 10^4$ μM).

Compound	*F. solani*	*A. niger*	*C. albicans*
[L]	18.7	19.1	18.8
[CuL(bpy)Cl_2]	7.3	6.9	5.7
[CoL(bpy)Cl_2]	7.8	6.7	8.2
[NiL(bpy)Cl_2]	10.1	9.5	8.7
[ZnL(bpy)Cl_2]	11.2	11.7	10.2
Gentamicin	3.1	2.8	2.7

that the binding energy of the [CuL(bpy)Cl_2] is higher than that of other complexes and the order of binding energy is as follows: [CuL(bpy)Cl_2] > [CoL(bpy)Cl_2] > [NiL(bpy)Cl_2] > [ZnL(bpy)Cl_2]. The biological efficacy including DNA binding, DNA cleavage and antimicrobial screening data is in the following order: [CuL(bpy)Cl_2] > [CoL(bpy)Cl_2] > [NiL(bpy)Cl_2] > [ZnL(bpy)Cl_2]. It clearly indicates that the docking score decreases when the biological activity increases. Hence, it shows that the examined docking score of the present complexes is higher than that of a few Schiff base metal complexes available in the literature [46].

4. Conclusion

A new and innovative hetrocylic Schiff base ligand which is capable of making metal complexes with enhanced pharmacological properties has been synthesized and characterized. A series of metal (Cu(II), Co(II), Ni(II) and Zn(II)) complexes have been synthesized from L and characterized by physicochemical, spectral and electrochemical techniques. The role of 2,2′-bipyridine as ancillary ligand would hopefully take the studied complexes as more bio-relevant. All the complexes have octahedral geometry except Cu(II) complex which has the same with distortion. The interaction of the complexes with DNA has been effectively examined and explored by electronic absorption, ethidium bromide displacement assay, viscosity measurements, cyclic voltammetry, differential pulse voltammetry and molecular docking analysis. These studies prove that CT DNA interaction of the complexes follows intercalation mode. The DNA cleavage activity of all the metal complexes with pUC19 DNA under aerobic conditions is efficient cleavage in the presence of oxidizing agent (H_2O_2). The anti-pathogenic screening indicates that these complexes are good antimicrobial agents against different organisms and standards. These biological findings from our study would be helpful in perceptive of DNA interaction exposed by metal complexes and may lead to develop novel metal based therapeutic drugs.

Acknowledgments

The authors express their heartfelt thanks to the College Managing Board, Principal, and Head of the Department of Chemistry, VHNSN College for providing necessary research facilities to complete this work successfully. The characterization facilities afforded by IIT Bombay and CDRI, Lucknow are gratefully acknowledged by all authors.

Appendix A. Supplementary data

Supplementary data to this article can be found online at http://dx.doi.org/10.1016/j.jphotobiol.2015.11.011.

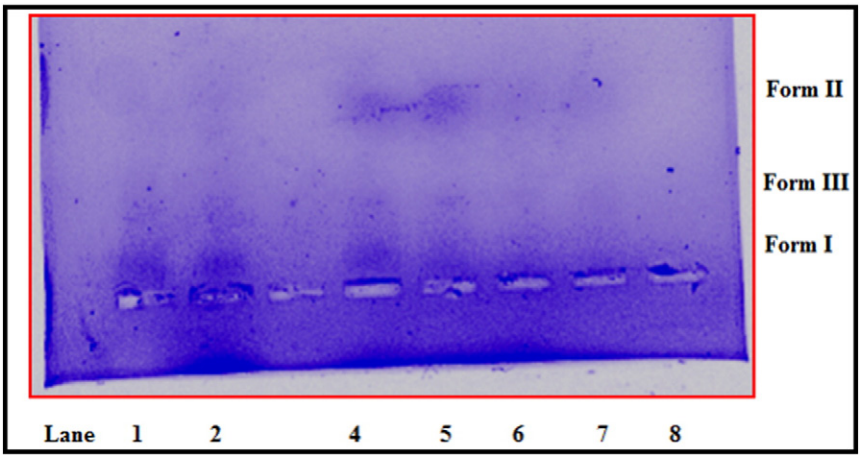

Fig. 6. The gel electrophoretic separation of plasmid pUC19 DNA treated with metal complexes. Lane 1; DNA control; Lane 2: DNA + ligand + H_2O_2; Lane 4: DNA + [CuL(bpy)Cl_2] + H_2O_2; Lane 5: DNA + [CoL(bpy)Cl_2] + H_2O_2; Lane 6: DNA + [NiL(bpy)Cl_2] + H_2O_2; Lane 7: DNA + [ZnL(bpy)Cl_2] + H_2O_2.

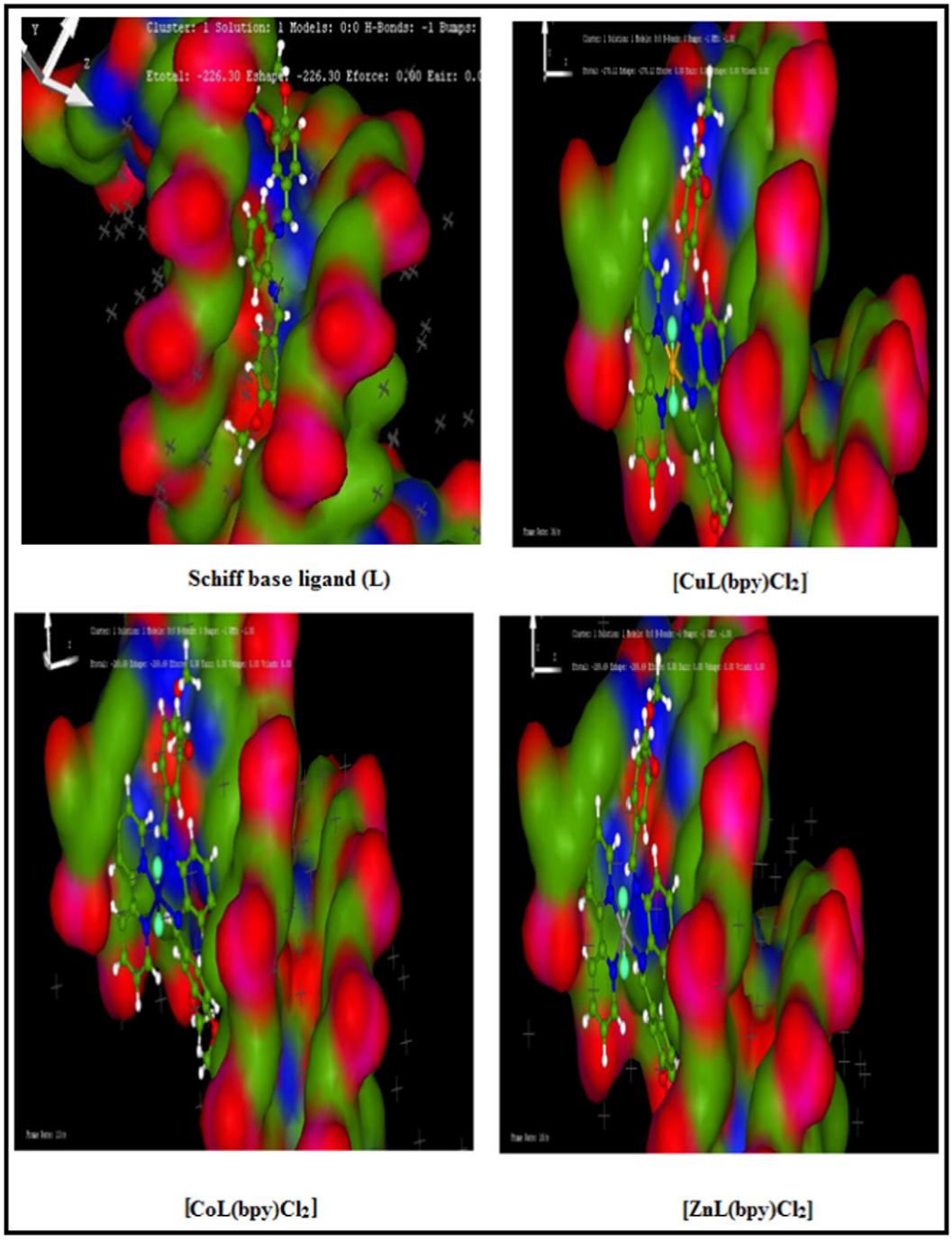

Fig. 7. Molecular docked model of L and its complexes with DNA.

References

[1] M. Nath, P.K. Saini, Chemistry and applications of organotin(IV) complexes of Schiff bases, Dalton Trans. 40 (2011) 7077–7121.

[2] P.G. Cozzi, Metal–salen Schiff base complexes in catalysis: practical aspects, Chem. Soc. Rev. 33 (2004) 410–421.

[3] N. Ananthi, U. Balakrishhnan, S. Velmathi, K.B. Manjunath, G. Umesh, Synthesis, characterization and third order non linear optical properties of metalloorganic chromophores, Opt. Photon. 2 (2012) 40–45.

[4] R. Antony, S.T.D. Manickam, P. Kollu, P.V. Chandrasekar, K. Karuppasamy, S. Balakumar, Highly dispersed Cu(II), Co(II) and Ni(II) catalysts covalently immobilized on imine-modified silica for cyclohexane oxidation with hydrogen peroxide, RSC Adv. 4 (2014) 24820–24830.

[5] G.G. Mohamed, M.M. Omar, A.A. Ibrahim, Biological activity studies on metal complexes of novel tridentate Schiff base ligand. Spectroscopic and thermal characterization, Eur. J. Med. Chem. 44 (2009) 4801–4812.

[6] A. Kundu, P.S. Hariharan, K. Prabakaran, S.P. Anthony, Developing new Schiff base molecules for selective colorimetric sensing of Fe^{3+} and Cu^{2+} metal ions: substituent dependent selectivity and colour change, Sensors Actuators B Chem. 206 (2015) 524–530.

[7] A.Y. Lukmantara, D.S. Kalinowski, N. Kumar, D.R. Richardson, Synthesis and biological evaluation of 2-benzoylpyridine thiosemicarbazones in a dimeric system: structure–activity relationship studies on their anti-proliferative and iron chelation efficacy, J. Inorg. Biochem. 141 (2014) 43–54.

[8] C. Rajarajeswari, M. Ganeshpandian, M. Palaniandavar, A. Riyasdeen, M.A. Akbarsha, Mixed ligand copper(II) complexes of 1,10-phenanthroline with tridentate phenolate/pyridyl/(benz)imidazolyl Schiff base ligands: covalent vs non-covalent DNA binding, DNA cleavage and cytotoxicity, J. Inorg. Biochem. 140 (2014) 255–268.

[9] H. Zafar, A. Ahmad, A.U. Khan, T.A. Khan, Synthesis, characterization and antimicrobial studies of Schiff base complexes, J. Mol. Struct. 1097 (2015) 129–135.

[10] R.R. Zaky, K.M. Ibrahim, H.M.A. El-Nadr, S.M. Abo-Zeid, Bivalent transition metal complexes of (E)-3-(2-benzylidenehydrazinyl)-3-oxo-N-(p-tolyl)propanamide: spectroscopic, computational, biological activity studies, Spectrochim. Acta A Mol. Biomol. Spectrosc. 150 (2015) 40–53.

[11] M. Shamsi, S. Yadav, F. Arjmand, Synthesis and characterization of new transition metal {Cu(II),Ni(II) and Co(II)}L-phenylalanine–DACH conjugate complexes:

in vitro DNA binding, cleavage and molecular docking studies, J. Photochem. Photobiol. B 136 (2014) 1–11.
[12] P. Gurumoorthy, D. Mahendiran, D. Prabhu, C. Krulvasu, A.K. Rahiman, Magneto-structural correlation, antioxidant, DNA interactions and growth inhibition activities of new chloro-bridged phenolate complexes, RSC Adv. 4 (2014) 42855–42872.
[13] G. Dehghan, J.E.N. Dolatabadi, A. Jouyban, K.A. Zeynali, S.M. Ahmadi, S. Kashanian, Spectroscopic studies on the interaction of quercetin–terbium(III) complex with calf thymus DNA, DNA Cell Biol. 30 (2010) 95–201.
[14] G. Zuber, J.C. Quada, S.M. Hecht, Sequence selective cleavage of a DNA octanucleotide by chlorinated bithiazoles and bleomycins, J. Am. Chem. Soc. 120 (1998) 9368–9369.
[15] N. Shahabadi, S. Mohammadi, Synthesis characterization and DNA interaction studies of a new Zn(II) complex containing different dinitrogen aromatic ligands, Bioinorg. Chem. Appl. 2012 (2012) 571913–571921.
[16] S. Anbu, S. Shanmugaraju, M. Kandaswamy, Electrochemical, phosphate hydrolysis, DNA binding and DNA cleavage properties of new polyaza macrobicyclic dinickel(II) complexes, RSC Adv. 2 (2012) 5349–5357.
[17] L.S. Lerman, Structural considerations in the interaction of DNA and acridines, J. Mol. Biol. 3 (1961) 18–14.
[18] Z.H. Chohan, M. Arif, M. Sarfraz, Metal-based antibacterial and antifungal amino acid derived Schiff bases: their synthesis, characterization and in vitro biological activity, Appl. Organomet. Chem. 21 (2007) 294–302.
[19] E. Mrkalić, A. Zianna, G. Psomas, M. Gdaniec, A. Czapik, E.C. Argyropoulou, M.L. Kantouri, Synthesis, characterization, thermal and DNA-binding properties of new zinc complexes with 2-hydroxyphenones, J. Inorg. Biochem. 134 (2014) 66–75.
[20] Z. Li, E. Badaeva, A. Ugrinov, S. Kilina, W. Su, Platinum chloride complexes containing 6-[9,9-Di(2-ethylhexyl)-7-R-9H-fluoren-2-yl]-2,2′-bipyridine ligand (RNO_2, CHO, Benzothiazol-2-yl,n-Bu, Carbazol-9-yl, NPh_2): tunable photophysics and reverse saturable absorption, Inorg. Chem. 52 (2013) 7578–7592.
[21] W.E. Estes, D.P. Gavel, W.B. Hatfield, D.J. Hodgson, Magnetic and structural characterization of dibromo- and dichlorobis(thiazole)copper(II), Inorg. Chem. 17 (1978) 1415–1421.
[22] R.K. Parashar, R.C. Sharma, Stability studies in relation to IR data of some Schiff base complexes of transition metals and their biological and pharmacological studies, Inorg. Chim. Acta 151 (1988) 201–208.
[23] M.B. Halli, R.B. Sumathi, Synthesis, spectroscopic, antimicrobial and DNA cleavage studies of new Co(II), Ni(II), Cu(II), Cd(II), Zn(II) and Hg(II) complexes with naphthofuran-2-carbohydrazide Schiff base, J. Mol. Struct. 1022 (2012) 130–138.
[24] M.S. El-Shahawi, A.F. Shoair, Synthesis, spectroscopic characterization, redox properties and catalytic activity of some ruthenium(II) complexes containing aromatic aldehyde and triphenylphosphine or triphenylarsine, Spectrochim. Acta A Mol. Biomol. Spectrosc. 60 (2004) 121–127.
[25] R. Antony, S.T.D. Manickam, K. Karuppasamy, P. Kollu, P.V. Chandrasekar, S. Balakumar, Organic–inorganic hybrid catalysts containing new Schiff base for environment friendly cyclohexane oxidation, RSC Adv. 4 (2014) 42816–42824.
[26] D. Kivelson, R. Neiman, ESR studies on the bonding in copper complexes, J. Chem. Phys. 35 (2004) 149–155.
[27] B.J. Hathaway, D.E. Billing, The electronic properties and stereochemistry of mononuclear complexes of the copper(II) ion, Coord. Chem. Rev. 5 (1970) 143–207.
[28] S. Tabassum, M. Zaki, F. Arjmand, New modulated design and synthesis of quercetin- Cu^{II}/Zn^{II}–Sn_2^{IV} scaffold as anticancer agents: in vitro DNA binding profile, DNA cleavage pathway and -I activity, Dalton Trans. 42 (2013) 10029–10041.
[29] H. Farrokhpour, H. Hadadzadeh, F. Darabi, F. Abyar, H.A. Rudbari, T. Ahmadi-Bagheri, A rare dihydroxo copper(II) complex with ciprooxacin; a combined experimental and ONIOM computational study of the interaction of the complex with DNA and BSA, RSC Adv. 4 (2014) 35390–35404.
[30] T. Kiran, V.G. Prasanth, M.M. Balamurali, C.S. Vasavi, P. Munusami, K.I. Sathyanarayanan, M. Pathak, Inorg. Chim. Acta 433 (2015) 26–34.
[31] W.D. Wilson, L. Ratmeyer, M. Zhao, L. Strekowski, D. Boykin, The search for structure-specific nucleic acid-interactive drugs: effects of compound structure on RNA versus DNA interaction strength, Biochemistry 32 (1993) 4098–4104.
[32] K. Nagaraj, G. Velmurugan, S. Sakthinathan, P. Venuvanalingam, S. Arunachalam, Influence of self-assembly on intercalative DNA binding interaction of double-chain surfactant Co(III) complexes containing imidazo[4,5-f][1,10]phenanthroline and dipyrido[3,2-d:2′-3′-f]quinoxaline ligands: experimental and theoretical study, Dalton Trans. 43 (2014) 18074–18086.
[33] V.A. Kawade, A.A. Kumbhar, A.S. Kumbhar, C. Nather, A. Erxleben, U.B. Sonawane, R.R. Joshi, Mixed ligand cobalt(II) picolinate complexes: synthesis, characterization, DNA binding and photocleavage, Dalton Trans. 40 (2011) 639–650.
[34] T. Arun, S. Packianathan, M. Malarvizhi, R. Antony, N. Raman, Bio-relevant complexes of novel N_2O_2 type heterocyclic ligand: synthesis, structural elucidation, biological evaluation and docking studies, J. Photochem. Photobiol. B Biol. 149 (2015) 93–102.
[35] M. Cory, D.D. Mckee, J. Kagan, D.W. Henry, J.A. Miller, Design, synthesis and DNA binding properties of bifunctional intercalators. Comparison of polymethylene and diphenyl ether chains connecting phenanthridine, J. Am. Chem. Soc. 107 (1985) 2528–2536.
[36] T. Arun, R. Subramanian, S. Packianathan, N. Raman, Fluorescence titrations of bio-relevant complexes with DNA: synthesis, structural investigation, DNA binding/cleavage, antimicrobial and molecular docking studies, J. Fluoresc. 25 (2015) 1127–1140.
[37] M.T. Carter, M. Rodriguez, A.J. Bard, Voltammetric studies of the interaction of metal chelates with DNA. 2. Tris-chelated complexes of cobalt (III) and iron (II) with 1, 10-phenanthroline and 2, 2′-bipyridine, J. Am. Chem. Soc. 111 (1989) 8901–8911.
[38] R.F. Brissos, E. Torrents, F.M.S. Mello, W.C. Pires, E.P. Silveira-Lacerda, A.B. Caballero, A. Caubet, C. Massera, O. Roubeau, S.J. Teat, P. Gamez, Highly cytotoxic DNA-interacting copper(II) coordination compounds, Metallomics 6 (2014) 1853–1868.
[39] P. Mendu, C.G. Kumari, R. Ragi, Synthesis, characterization, DNA binding, DNA cleavage and antimicrobial studies of Schiff base ligand and its metal complexes, J. Fluoresc. 25 (2015) 369–378.
[40] A.A. El-Sherif, M.M. Shoukry, M.M.A. Abd-Elgawad, Synthesis, characterization, biological activity and equilibrium studies of metal(II) ion complexes with tridentate hydrazone ligand derived from hydralazine, Spectrochim. Acta A Mol. Biomol. Spectrosc. 98 (2012) 307–321.
[41] B.G. Tweedy, Plant extracts with metal ions as potential antimicrobial agents, Phytopathology 25 (1964) 910–914.
[42] J. Lakshmipraba, S. Arunachalam, R.V. Solomon, P. Venuvanalingam, A. Riyasdeen, R. Dhivya, M.A. Akbarsha, Surfactant–copper(II) Schiff base complexes: synthesis, structural investigation, DNA interaction, docking studies, and cytotoxic activity, J. Biomol. Struct. Dyn. 33 (2015) 877–891.
[43] S. Tabassum, S. Yada, Investigation of diorganotin(IV) complexes: Synthesis, characterization, in vitro DNA binding studies and cytotoxicity assessment of di-n-butyltin(IV)complex, Inorg. Chim. Acta 423 (2014) 204–214.
[44] G. Barone, A. Terenzi, A. Lauria, A.M. Almerico, J.M. Leal, L. Busto, B. García, DNA-binding of nickel(II), copper(II) and zinc(II) complexes: structure–affinity relationships, Coord. Chem. Rev. 257 (2013) 2848–2862.
[45] P. Arthi, S. Shobana, P. Srinivasan, L. Mitu, A.K. Rahiman, Synthesis, characterization, biological evaluation and docking studies of macrocyclic binuclear manganese(II) complexes containing 3,5-dinitrobenzoyl pendant arms, Spectrochim. Acta A Mol. Biomol. Spectrosc. 143 (2015) 49–58.
[46] A. Lauria, R. Bonsignore, A. Terenzi, A. Spinello, F. Giannici, A. Longo, A.M. Almerico, G. Barone, Nickel(II), copper(II) and zinc(II) metallo-intercalators: structural details of the DNA-binding by a combined experimental and computational investigation, Dalton Trans. 43 (2014) 6108–6119.